Advances in Nanoparticles, 2016, 5, 167-175
Published Online August 2016 in SciRes. http://www.scirp.org/journal/anp
http://dx.doi.org/10.4236/anp.2016.53018

Scientific Research Publishing

PtAg Nanoparticle Electrocatalysts for the Glycerol Oxidation Reaction in Alkaline Medium

Binh Thi Xuan Lam, Masanobu Chiku, Eiji Higuchi, Hiroshi Inoue

Department of Applied Chemistry, Graduate School of Engineering, Osaka Prefecture University, Osaka, Japan
Email: inoue-h@chem.osakafu-u.ac.jp

Received 23 June 2016; accepted 22 July 2016; published 25 July 2016

Abstract

To improve the activity for glycerol oxidation reaction (GOR) of Pt, PtAg (mole ratio of Pt/Ag = 3 and 1) alloy nanoparticle-loaded carbon black (Pt/CB, PtAg(3:1)/CB, PtAg(1:1)/CB) catalysts were prepared by a wet method. The resultant catalysts, moreover, were heat-treated in a N_2 atmosphere at 200˚C. The alloying of Pt with Ag for each PtAg/CB was confirmed by X-ray diffractometry and electron dispersive X-ray spectrometry. The heat-treatment did not change the crystal structure of the PtAg alloys and increased their particle size. X-ray photoelectron spectroscopy exhibited that stabilizers were completely removed from the PtAg alloy surface, and the Pt4f and Ag3d doublets due to metallic Pt and Ag, respectively, shifted to lower binding energies, supporting the alloying of Pt with Ag. Both PtAg/CB electrodes had two oxidation waves of glycerol irrespective of heat-treatment, which was different from the Pt/CB electrode. The onset potential of the first oxidation wave was −0.60 V, which was 0.20 V less positive than that for the Pt/CB electrode, indicating the alloying of Pt with Ag greatly improved the GOR activity of Pt. The heat-treated PtAg(3:1)/CB electrode improved the GOR current density of the second oxidation peak. In the potentiostatic electrolysis at −0.1 and 0 V for both PtAg/CB electrodes, the ratio of oxidation current density at 60 min to that at 5 min (j_{60}/j_5), an indicator of the catalyst deterioration, at 0 V was higher than that at −0.1 V, because the adsorbed oxidation intermediates were greatly consumed at the larger overpotential. The heat-treatment of the PtAg(3:1)/CB electrode increased the j_{60}/j_5 value at −0.1 V but decreased that at 0 V. This could be attributed to the formation of high-order oxidation intermediates which might have stronger poisoning effect.

Keywords

Glycerol Oxidation Reaction, Direct Glycerol Fuel Cell, PtAg Alloy, Bi-Functional Effect

How to cite this paper: Lam, B.T.X., Chiku, M., Higuchi, E. and Inoue, H. (2016) PtAg Nanoparticle Electrocatalysts for the Glycerol Oxidation Reaction in Alkaline Medium. *Advances in Nanoparticles*, **5**, 167-175.
http://dx.doi.org/10.4236/anp.2016.53018

1. Introduction

Biodiesel fuel (BDF) is known as a carbon-neutral fuel which is produced with glycerol byproduct through the transesterification of vegetable fats and oils or long-chain alkyl esters with methanol. The production of BDF is on the increase, so new application of the increasing glycerol byproduct is an important and urgent issue. Direct alcohol fuel cells (DAFCs) have attracted considerable interest because the alcohols such as methanol and ethanol as a fuel have a high energy density and are easy to handle, store, and transport compared with pure hydrogen [1]-[4]. The use of the glycerol byproduct for DAFCs is promising, because they are expected to produce electricity with a low environmental load and high energy conversion efficiency.

Palladium is less expensive than gold and platinum, and less active for GOR in alkaline media than platinum. So the alloying of Pd with various foreign metals has been attempted for improving its GOR activity [5]-[7]. We also developed the Pd-Ag and Pd-Au alloy nanoparticle catalysts by a wet method at room temperature, and found that the alloying of Pd with Ag was effective for making the onset potential of the GOR current (E_{onset}) lower, whereas the alloying with Au made the maximum GOR current higher [8]. In particular, the PdAg nanoparticle-loaded carbon black whose the Pd/Ag mole ratio was 3 succeeded in reducing the E_{onset} by 0.15 V compared to the Pd nanoparticle-loaded CB, which was comparable to the E_{onset} of Pt. To lower the E_{onset} of Pt or reduce the overpotential for GOR in alkaline media, the alloying of Pt with foreign metals should be significantly useful, but, to our knowledge, there have been only a few researches with $Pt_{84}Ru_{16}$, $Pt_{88}Ru_6Sn_6$, $Pt_{96}Sn_4$ [9], Pt_xNi (x = 1 - 3) [10]. PtAg alloys have also been used for various alcohol oxidation reactions in alkaline media, but as for GOR only one paper has been published [11], and described that Pt was deposited on Ag nanowires by the partial galvanic displacement, and the alloying of Pt with Ag also occurred during the Pt deposition to form the PtAg nanoparticles which were superior in GOR activity and durability to Pt black [11]. However, this method seems to be difficult to control the alloy composition and particle size. In the present study, we used the wet nanoparticle preparation method, which was also used for the preparation of PdAg/CB [8] and Pt/CB and Pd/CB [12], to prepare PtAg alloy nanoparticle-loaded CB (PtAg/CB) catalysts with different Pt/Ag mole ratios, and evaluate their GOR activity in alkaline medium. In addition, the effect of heat treatment of the PtAg/CB catalysts on the GOR activity and tolerance to poisoning was investigated.

2. Experimental

A solution of KBH_4 (4 mmol) as a reducing agent in H_2O (1.5 mL) was added dropwise to a solution containing $PtCl_2$ (0.5 or 0.75 mmol) and AgCl (0.5 or 0.25 mmol) and $N(Oct)_4Br$ (4 mmol) in THF (150 mL) with stirring at 1800 rpm at 30˚C in an Ar atmosphere. Each reaction mixture was still stirred at the same rate for 30 min, resulting in a black colloidal suspension. The suspended solid was isolated by suction filtration in air and washed with excess H_2O, acetone, and ethanol at room temperature, yielding a black waxy solid. The black solid was redispersed in ethanol. Ketjen black (67 mg) was added in the dispersion and sonicated for 10 min. After suction filtration, the residue was redispersed in 300 mL of 0.1 M $HClO_4$ aqueous solution and then sonicated for 10 min. After suction filtration, the residue was washed with excess H_2O, acetone, and ethanol at room temperature. The resultant powder is called PtAg(1:1)/CB or PtAg(3:1)/CB hereafter. The Pt/CB, Ag/CB powders were also prepared by the same procedure. The heat-treatment of PtAg(3:1)/CB and PtAg(1:1)/CB was performed in a N_2 atmosphere at 200˚C for 15 min.

To evaluate the metal loading in each catalyst, thermogravimetry was performed in air by heating from room temperature to 700˚C at a rate of 1 $K \cdot min^{-1}$. The metal or alloy loading on CB was 50, 55, 55 and 50 wt% for Pt/CB, heat-treated PtAg(3:1)/CB, heat-treated PtAg(1:1)/CB and Ag/CB, respectively.

Structure and average size of metal or alloy nanoparticles for each catalyst were performed using an X-ray diffractometry (XRD) and electron dispersive X-ray (EDX) spectrometry. Chemical state of Pt and Ag in each catalyst was measured by X-ray photoelectron spectroscopy (XPS). The X-ray source was Mg Kα at 1253.6 eV operating at 10 kV and 20 mA. The base pressure of the system was 1.3×10^{-7} Pa.

The modification of each catalyst on a glassy carbon (GC) substrate (5 mmϕ) was performed according to Ref. [13]. The amount of each catalyst loaded on the GC was 12.8 $\mu g \cdot cm^{-2}$. A 0.05 wt% Nafion solution (Sigma Aldrich) in ethanol (10 µL) was cast on the dried catalyst layer, and then heat-treated in air at 120˚C for 1 h to evaporate ethanol, resulting in a catalyst electrode thinly coated with a thin 0.1-µm-thick Nafion film. A Pt plate and an Hg/HgO/1 M KOH electrode were used as the counter and reference electrodes, respectively. The GOR activity and durability of each electrode were evaluated in 1 M KOH with and without 0.5 M glycerol at room

temperature by cyclic voltammetry and potentiostatic electrolysis.

3. Results and Discussion

3.1. Structure of PtAg Nanoparticle-Loaded Carbon Black Catalysts with and without Heat-Treatment

Figure 1 shows XRD patterns for Pt/CB, PtAg(3:1)/CB and PtAg(1:1)/CB with and without heat-treatment, and Ag/CB. In each XRD pattern, a small broad diffraction peak at 20˚ - 25˚ was assigned to the (002) plane of CB with a hexagonal structure [13]. Moreover, each XRD pattern had diffraction peaks assigned to the face-centered cubic (fcc) structure [14] [15]. For PtAg(3:1)/CB and PtAg(1:1)/CB without heat-treatment, each diffraction peak was broad and shifted to lower angles than that for Pt/CB, and the width of peak shift was increased with the Ag content, suggesting the formation of alloy nanoparticles of Pt and Ag. The mole ratio of Pt/Ag estimated by using Vegard's law was 3.0 and 1.0 for PtAg(3:1)/CB and PtAg(1:1)/CB, respectively, which were equivalent to those evaluated by EDX spectrometry and the molar concentration ratios of the Pt and Ag precursors, suggesting that the bulk composition of the present PtAg nanoparticles was controllable with the mixing ratio of the Pt and Ag precursors. After the heat-treatment of PtAg(3:1)/CB and PtAg(1:1)/CB, each diffraction peak became sharp without any angle shift, suggesting that the size of the PtAg alloy nanoparticles increased. In both cases the mean crystallite size of the PtAg particles loaded on CB estimated by using Scherrer's equation increased from 2.1 to 4.0 nm after the heat-treatment.

XPS analysis for all catalysts did not show any peaks in the N1s and the Br3d core level spectra, suggesting that the $N(Oct)_4Br$ stabilizer was completely removed by washing with H_2O, ethanol, acetone, and $HClO_4$ solution.

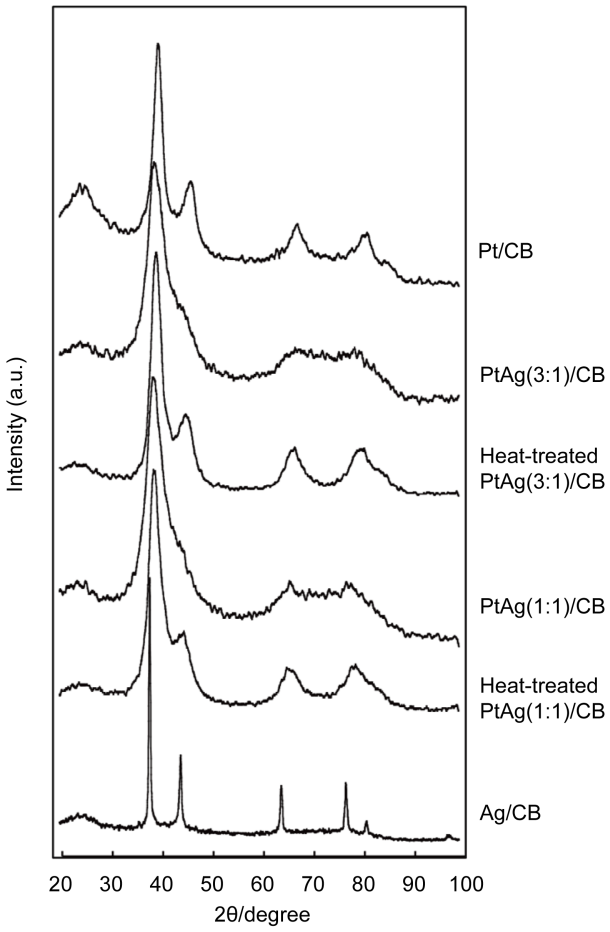

Figure 1. XRD patterns for Pt/CB, PtAg(3:1)/CB, PtAg(1:1)/CB, heat-treated PtAg(3:1)/CB, heat-treated PtAg(1:1)/CB and Ag/CB.

The Pt4f and Ag3d core level spectra for each catalyst are shown in **Figure 2**. Pt/CB and Ag/CB exhibited intense doublets assigned to metallic Pt and Ag [16] in the Pt4f and Ag3d core level spectra, respectively. The Pt4f doublets and Ag3d doublets for PtAg(3:1)/CB and PtAg(1:1)/CB shifted to lower binding energies than those for Pt/CB and Ag/CB due to the alloying of Pt with Ag, which was consistent with the previous report [17]. This trend was maintained even after heat-treatment.

3.2. Electrochemical Properties and Glycerol Oxidation Reaction Activity for PtAg Nanoparticle-Loaded Carbon Black Catalysts with and without Heat-Treatment

Figure 3(a) shows cyclic voltammograms (CVs) of Nafion-coated PtAg(3:1)/CB and PtAg(1:1)/CB with and without heat-treatment, Pt/CB and Ag/CB electrodes in an Ar-saturated 1 M KOH solution. In the CV of the Pt/CB electrode, two couples of butterfly peaks owing to hydrogen adsorption/desorption [12] were observed in the potential range below −0.4 V vs Hg/HgO, and the oxidation current due to the surface Pt-OH_{ad} formation [18] [19] began to flow around −0.4 V in the forward sweep and its reduction current had a peak around −0.15 V in the backward sweep. The electrochemical surface area (ECSA) of Pt/CB was evaluated as 0.36 cm^2 from the electric charge for the hydrogen desorption, assuming charge density of 210 $\mu C \cdot cm^{-2}$ for polycrystalline Pt [20]. The Ag/CB electrode did not have any redox peaks for hydrogen adsorption/desorption, and a couple of redox peaks for the Ag_2O formation/reduction was observed around 0.28 V and 0.18 V. The ECSA of Ag/CB was evaluated as 0.29 cm^2 from the electric charge for the reduction of the surface Ag_2O, assuming charge density of 420 $\mu C \cdot cm^{-2}$ for polycrystalline Ag [20].

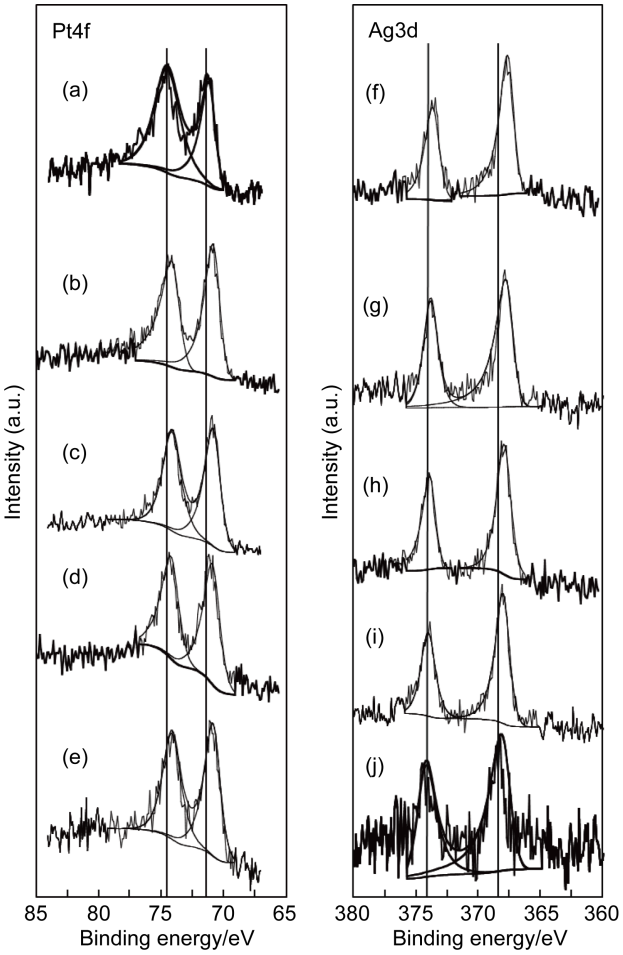

Figure 2. Pt4f and Ag3d core level spectra for (a) Pt/CB, (b), (f) PtAg(3:1)/CB, (c), (g) heat-treated PtAg(3:1)/CB, (d), (h) PtAg(1:1)/CB and (e), (i) heat-treated PtAg(1:1)/CB and (j) Ag/CB.

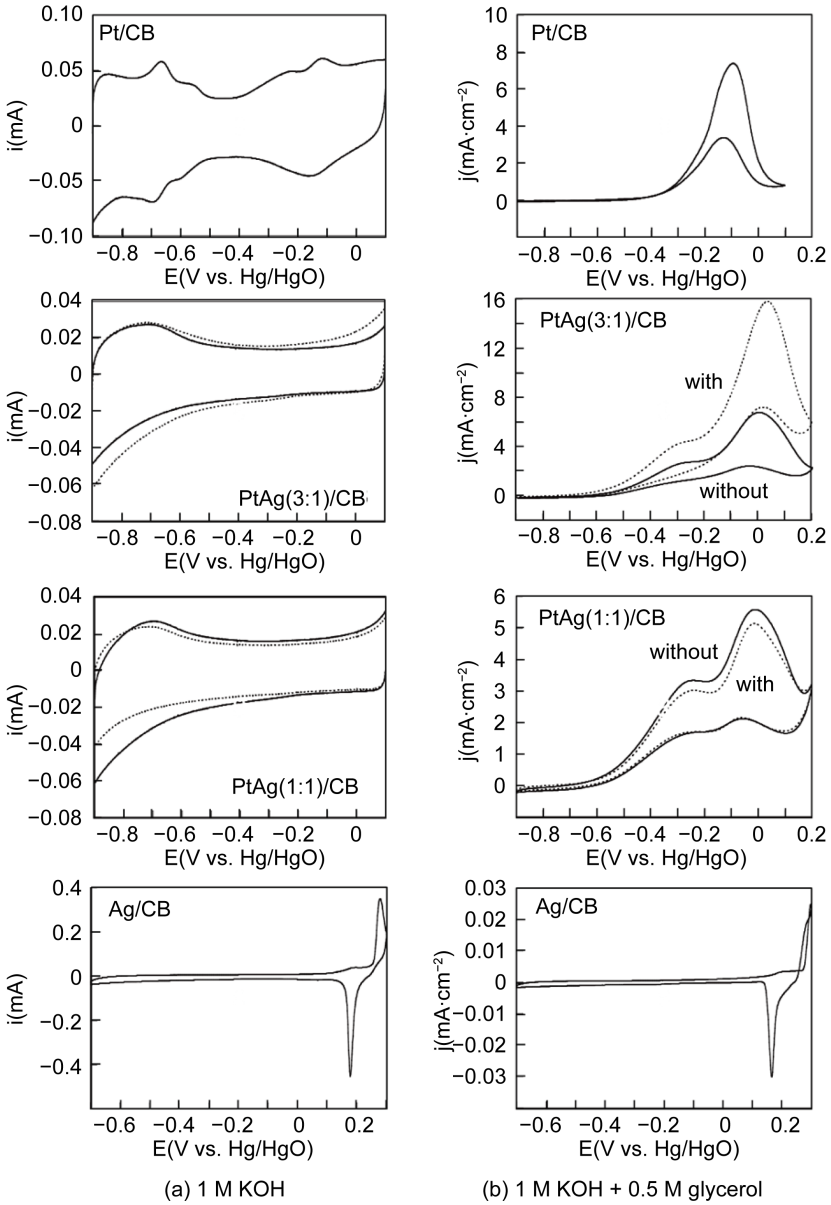

Figure 3. CVs of Pt/CB, PtAg(3:1)/CB, heat-treated PtAg(3:1)/CB, PtAg(1:1)/CB, heat-treated PtAg(1:1)/CB and Ag/CB electrodes in Ar-saturated (a) 1 M KOH and (b) (1 M KOH + 0.5 M glycerol) solutions. Sweep rate = 20 $mV \cdot s^{-1}$.

For the PtAg(3:1)/CB and PdAg(1:1)/CB electrodes, irrespective of the Ag content and heat-treatment, two couples of butterfly waves for hydrogen adsorption/desorption changed to broad irreversible waves, and the onset potential of the oxidation current due to the surface Pt-OH_{ad} formation greatly shifted to higher potentials, which seemed to indicate that the corner and edge sites on the PtAg nanoparticle surfaces were occupied by Ag atoms. The ECSAs of the surface Pt site for the PtAg(3:1)/CB and PdAg(1:1)/CB electrodes were estimated as 0.14 and 0.10 cm^2, respectively, regardless of heat-treatment. Since the sizes of the heat-treated PtAg(3:1) and PtAg(1:1) particles are similar to the size (3.8 nm) of the Pt particles, the ECSA of the surface Pt site is estimated as three quarter (0.27 cm^2) for the PtAg(3:1)/CB and a half (0.18 cm^2) for the PtAg(1:1)/CB compared to the ECSA of Pt/CB if the surface composition is equivalent to the bulk composition. The experimental ECSAs are smaller than the estimated ones, suggesting that the PtAg particle surfaces are Ag-enriched compared to the bulk compositions.

Figure 3(b) shows CVs of Nafion-coated PtAg(3:1)/CB and PtAg(1:1)/CB with and without heat-treatment, Pt/CB and Ag/CB electrodes in an Ar-saturated (1.0 M KOH + 0.5 M glycerol) solution. All current densities are shown as current per unit ECSA of Pt for Pt/CB and PtAg/CB with and without heat-treatment, and that per unit ECSA of Ag for Ag/CB. The Ag/CB electrode was inactive for GOR in the alkaline medium. The current for GOR at the Pt/CB electrode began to flow around −0.4 V, which was connected with the Pt-OH_{ad} formation as shown in **Figure 3(a)**, suggesting that GOR at Pt/CB followed the bi-functional mechanism, where GOR was accelerated by glycerol molecules dissociatively adsorbed on the surface Pt atoms coupling with OH_{ad} formed on the adjacent Pt atoms. Moreover, the peak potential of the GOR current density was observed around −0.1 V, whereas in the backward sweep oxidation current began to flow around 0 V again. In the forward sweep the fresh Pt surface for GOR decreased as the coverage of Pt-OH_{ad} increased and some carbonaceous intermediates, which were strongly adsorbed and difficult to remove, caused the appearance of the oxidation peak. In the backward sweep, the fresh surface was recovered by the reduction of Pt-OH_{ad} and the residual poisoning intermediates were oxidatively removed again, leading to the appearance of the oxidation current. These results were also observed in the CV for GOR at the Pd/CB electrode [8].

For the PtAg(3:1)/CB and PtAg(1:1)/CB electrodes, two oxidation waves for GOR were observed irrespective of heat-treatment. In both electrodes the first oxidation wave with the lower potential had the onset potential around ca. −0.6 V, which was 0.20 V less positive than that for the Pt/CB electrode. The appearance of the first oxidation wave, however, was more negative than the onset potential of the Pt-OH_{ad} formation in contrast to the Pt/CB electrode. The electronic modification of Pt based on its alloying with Ag may activate adsorbed glycerol. Also, Ag is known to promote the removal of adsorbed CO or similar poisoning intermediates out of the PdAg surface [21] [22], which seems to cause a positive shift of the second oxidation peak potential.

The GOR current density for the PtAg(3:1)/CB electrode was increased after the heat-treatment, whereas that for the PtAg(1:1)/CB electrode was not influenced by the heat-treatment. In the CV of the heat-treated PtAg(3:1)/CB electrode in a 1 M KOH solution, the onset potential for the formation of Pt-OH_{ad} was observed at more negative potential than that before the heat-treatment, as shown in **Figure 3(a)**, which seems to cause the great increase in the second oxidation wave with the higher peak potential due to the increase in bi-functional effect.In addition, the redox waves below −0.4 V for the PtAg(3:1)/CB electrode a little increased after the heat-treatment, as shown in **Figure 3(a)**. The Ag atoms at the corner and edge sites of the PdAg(3:1) nanoparticle surface might partially move during heat-treatment to expose the Pt atoms.

3.3. Tolerance to Poisoning for PtAg Nanoparticle-Loaded Carbon Black Catalysts with and without Heat-Treatment

Figure 4 shows the time courses of oxidation current density at −0.1 and 0 V in an Ar-saturated (1.0 M KOH + 0.5 M glycerol) solution for PtAg(3:1)/CB and PtAg(1:1)/CB with and without heat-treatment and Pt/CB electrodes. In this figure, all current densities are shown as current per unit ECSA of Pt. For the Pt/CB electrode, the oxidation current density sharply decreased over time after the initial drop owing to double-layer charging owing to the poisoning of the active sites with the adsorbed carbonaceous intermediates. The ratio of oxidation current density at 60 min to that at 5 min (j_{60}/j_5) was evaluated as an indicator of the catalyst deterioration, and the results are shown in **Figure 5**. For the PtAg(3:1)/CB, PtAg(1:1)/CB and Pt/CB electrodes, the j_{60}/j_5 value at 0 V was larger than that at −0.1 V, indicating the catalyst deterioration was suppressed at the larger overpotential. After the heat-treatment, the potential dependence of the j_{60}/j_5 value for the PtAg(3:1)/CB was different from that for the PtAg(1:1)/CB electrode. In each case the GOR intermediates formed in the first oxidation wave seemed to be additionally oxidized by the bi-functional effect at larger overpotentials to reduce the poisoning.However, the heat-treatment of the PtAg(3:1)/CB electrode increased the j_{60}/j_5 value at −0.1 V but decreased that at 0 V. For this catalyst, the second oxidation peak current density greatly increased, as shown in **Figure 3(b)**, accelerating the oxidation of adsorbed GOR intermediates. This, however, can lead to the formation of high-order oxidation intermediates which may have stronger poisoning effect. The identification of the intermediates formed in GOR on the PtAg nanoparticle surface is the next step to elucidate the GOR mechanism, and is underway.

4. Conclusions

Two PtAg (mole ratio of Pt/Ag = 3 and 1) alloy nanoparticle-loaded CB catalysts for GOR in alkaline medium

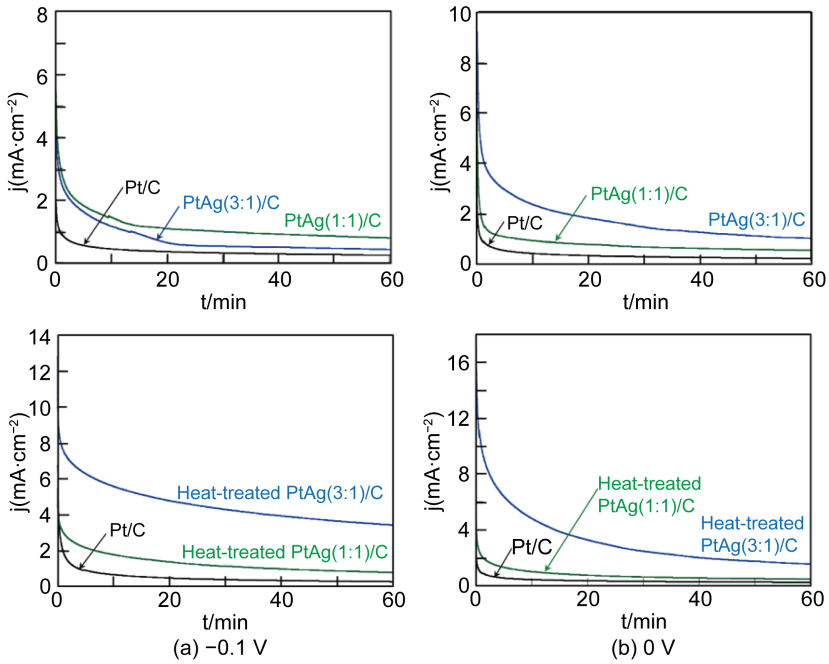

Figure 4. Time courses of oxidation current density in electrostatic electrolysis at (a) −0.1 V and (b) 0 V vs. Hg/HgO for Pt/CB, PtAg(3:1)/CB, PtAg(1:1)/CB, heat-treated PtAg(3:1)/CB and heat-treated PtAg(1:1)/CB electrodes in Ar-saturated (1 M KOH + 0.5 M glycerol) solution.

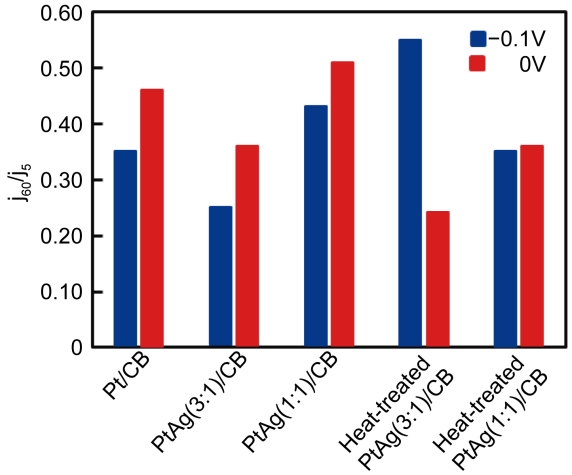

Figure 5. j_{60}/j_5 values at −0.1 V and 0 V for Pt/CB, PtAg(3:1)/CB, PtAg(1:1)/CB, heat-treated PtAg(3:1)/CB and heat-treated PtAg(1:1)/CB electrodes.

were prepared by a wet method at room temperature. Also, the resultant catalysts were heat-treated in N_2 atmosphere at 200˚C. The alloying of Pt with Ag for each PtAg/CB was confirmed by XRD and EDX spectrometry. The heat-treatment did not change the crystal structure of the PtAg alloys and increased their particle size. XPS data exhibited that stabilizers were completely removed from the PtAg alloy surface, and the Pt4f and Ag3d doublets due to metallic Pt and Ag, respectively, shifted to lower binding energies, supporting the alloying of Pt with Ag.

Both PtAg/CB electrodes had two oxidation waves of glycerol irrespective of heat-treatment, which was different from the Pt/CB electrode. The onset potential of the first oxidation wave was −0.60 V, which was 0.20 V less positive than that for the Pt/CB electrode, indicating the alloying of Pt with Ag greatly improved the GOR activity of Pt. The heat-treated PtAg(3:1)/CB electrode could increase the GOR current density of the second

oxidation peak. In the potentiostatic electrolysis at −0.1 and 0 V for the PtAg(3:1)/CB and PtAg(1:1)/CB electrodes, the j_{60}/j_5 value at 0 V as an indicator of the catalyst deterioration was higher than that at −0.1 V, because the adsorbed oxidation intermediates were greatly consumed at the larger overpotential. The heat-treatment of the PtAg(3:1)/CB electrode increased the j_{60}/j_5 value at −0.1 V but decreased that at 0 V. This could be attributed to the formation of high-order oxidation intermediates which might have stronger poisoning effect.

Acknowledgements

This work was partially supported by JSPS KAKENHI Grant Number 15H04162.

References

[1] Kakati, N., Maiti, J., Lee, S.H., Viswanathan, B. and Yoon, Y.S. (2014) Anode Catalysts for Direct Methanol Fuel Cells in Acidic Media: Do We Have Any Alternative for Pt or Pt-Ru? *Chemical Review*, **114**, 12397-12429. http://dx.doi.org/10.1021/cr400389f

[2] Antolini, E. (2007) Catalysts for Direct Ethanol Fuel Cells. *Journal of Power Sources*, **170**, 1-12. http://dx.doi.org/10.1016/j.jpowsour.2007.04.009

[3] Lamy, C., Rousseau, S., Belgsir, E.M., Countanceau, C. and Léger, J. (2004) Recent Progress in the Direct Ethanol Fuel Cell: Development of New Platinum-Tin Electrocatalysts. *Electrochimica Acta*, **49**, 3901-3908. http://dx.doi.org/10.1016/j.electacta.2004.01.078

[4] Behr, A., Eilting, J., Irawadi, K., Leschinski, J. and Lindner, F. (2008) Improved Utilisation of Renewable Resources: New Important Derivatives of Glycerol. *Green Chemistry*, **10**, 13-30. http://dx.doi.org/10.1039/B710561D

[5] Simões, M., Baranton, S. and Coutanceau, C. (2010) Electro-Oxidation of Glycerol at Pd Based Nano-Catalysts for an Application in Alkaline Fuel Cells for Chemicals and Energy Cogeneration. *Applied Catalysis B*: *Environmental*, **93**, 354-362. http://dx.doi.org/10.1016/j.apcatb.2009.10.008

[6] Mougenot, M., Caillard, A., Simoes, M., Baraton, S., Coutanceau, C. and Brault, P. (2011) PdAu/C Catalysts Prepared by Plasma Sputtering for the Electro-Oxidation of Glycerol. *Applied Catalysis B*, **107**, 372-379. http://dx.doi.org/10.1016/j.apcatb.2011.07.039

[7] Holade, Y., Morais, C., Arrii-Clacens, S., Servat, K., Napporn, T.W. and Kokoh, K.B. (2013) New Preparation of PdNi/C and PdAg/C Nanocatalysts for Glycerol Electrooxidation in Alkaline Medium. *Electrocatalysis*, **4**, 167-178. http://dx.doi.org/10.1007/s12678-013-0138-1

[8] Lam, B.T.X., Chiku, M., Higuchi, E. and Inoue, H. (2015) Preparation of PdAg and PdAu Nanoparticle-Loaded Carbon Black Catalysts and Their Electrocatalytic Activity for the Glycerol Oxidation Reaction in Alkaline Medium. *Journal of Power Sources*, **297**, 149-157. http://dx.doi.org/10.1016/j.jpowsour.2015.07.086

[9] Falase, A., Garcia, K., Main, M., Lau, C. and Atanassov, P. (2012) Electrooxidation of Ethylene Glycol and Glycerol by Platinum-Based Binary and Ternary Nano-Structured Catalysts. *Electrochimica Acta*, **66**, 295-301. http://dx.doi.org/10.1016/j.electacta.2012.01.096

[10] Lee, S., Kim, H.J., Choi, S.M., Seo, M.H. and Kim, W.B. (2012) The Promotional Effect of Ni on Bimetallic PtNi/C Catalysts for Glycerol Electrooxidation. *Applied Catalysis A: General*, **429-430**, 39-47. http://dx.doi.org/10.1016/j.apcata.2012.04.002

[11] Kim, Y., Kim, H. and Kim, W.B. (2014) PtAg Nanotubes for Electrooxidation of Ethylene Glycol and Glycerol in Alkaline Media. *Electrochemistry Communications*, **46**, 36-39. http://dx.doi.org/10.1016/j.elecom.2014.06.007

[12] Lam, B.T.X., Chiku, M., Higuchi, E. and Inoue, H. (2016) Rhodium Nanoparticle-Loaded Carbon Black Electrocatalyst for the Glycerol Oxidation Reaction in Alkaline Medium. *Advances in Nanoparticles*, **5**, 60-66. http://dx.doi.org/10.4236/anp.2016.51007

[13] Higuchi, E., Miyata, K., Takase, T. and Inoue, H. (2011) Ethanol Oxidation Reaction Activity of Highly Dispersed Pt/SnO_2 Double Nanoparticles on Carbon Black. *Journal of Power Sources*, **196**, 1730-1737. http://dx.doi.org/10.1016/j.jpowsour.2010.10.008

[14] Antolini, E. and Cardellini, F. (2011) Formation of Carbon Supported PtRu Alloys: An XRD Analysis. *Journal of Alloys and Compounds*, **315**, 118-122. http://dx.doi.org/10.1016/S0925-8388(00)01260-3

[15] Simões, M., Baranton, S. and Coutanceau, C. (2011) Enhancement of Catalytic Properties for Glycerol Electrooxidation on Pt and Pd Nanoparticles Induced by Bi Surface Modification. *Applied Catalysis B*: *Environmental*, **110**, 40-49. http://dx.doi.org/10.1016/j.apcatb.2011.08.020

[16] Moulder, J.F., Stickle, W.F., Sobol, P.E. and Bomben, K.D. (1995) Handbook of X-Ray Photoelectron Spectroscopy. Physical Electronics, Inc., Chanhassen.

[17] Dong, S.Z., Xiao, F.H. and Deng, J.F. (1988) The Adsorption of Oxygen and the Oxidation of Methanol on Silver-Platinum Alloys. *Journal of Catalysis*, **109**, 170-179. http://dx.doi.org/10.1016/0021-9517(88)90195-9

[18] Concha, B.M. and Chatenet, M. (2009) Direct Oxidation of Sodium Borohydride on Pt, Ag and Alloyed Pt-Ag Electrodes in Basic Media. Part I: Bulk Electrodes. *Electrochimica Acta*, **54**, 6119-6129. http://dx.doi.org/10.1016/j.electacta.2009.05.027

[19] Guerra-Balcázar, M., Cuevas-Muniz, F.M., Álvarez-Contreras, L., Arriaga, L.G. and Ledesma-García, J. (2012) Evaluation of Bimetallic Catalyst PtAg/C as a Glucose-Tolerant Oxygen Reduction Cathode. *Journal of Power Sources*, **197**, 121-124. http://dx.doi.org/10.1016/j.jpowsour.2011.09.051

[20] Zhang, Z., Xin, L., Qi, J., Chadderdon, D.J. and Li, W. (2013) Supported Pt, Pd and Au Nanoparticle Anode Catalysts for Anion-Exchange Membrane Fuel Cells with Glycerol and Crude Glycerol Fuels. *Applied Catalysis B*: *Environmental*, **136-137**, 29-39. http://dx.doi.org/10.1016/j.apcatb.2013.01.045

[21] Holade, Y., Morais, C., Arrii-Clacens, S., Servat, K., Napporn, T.W. and Kokoh, K.B. (2013) Toward the Electrochemical Valorization of Glycerol: Fourier Transform Infrared Spectroscopic and Chromatographic Studies. *ACS Catalysis*, **3**, 2403-2411. http://dx.doi.org/10.1021/cs400559d

[22] Wang, Y., Sheng, Z.M., Yang, H., Jiang, S.P. and Li, C.M. (2010) Electrocatalysis of Carbon Black- or Activated Carbon Nanotubes-Supported Pd-Ag towards Methanol Oxidation in Alkaline Media. *International Journal of Hydrogen Energy*, **35**, 10087-10093. http://dx.doi.org/10.1016/j.ijhydene.2010.07.172